研 究 速 報

Coupled Finite Element Analysis of Magneto-Superelastic Behaviors of Ferromagnetic Shape Memory Alloy Helical Springs

Yutaka TOI*, Jong-Bin LEE* and Minoru TAYA**

1. Introduction

Ferromagnetic shape memory alloy (abbreviated as FSMA) is under development and is expected as a new material of SMA actuators. The coupled finite element analysis is conducted for the magneto-superelastic behavior of FSMA helical springs in the present study. The commercial code ANSYS/Emag and the superelastic analysis program developed by the authors[1,2] are used for the magnetic analysis and the superelastic analysis, respectively. The coupled calculation is conducted by the sequential approach (the loosely-coupled approach) as shown in Fig. 1.

2. Coupled Magneto-Superelastic Analysis of FSMA

2.1 Magnetic Analysis

The commercial code ANSYS/Emag is used for magnetic analysis. The method of difference scalar potential is employed with eight-noded hexahedron elements for magnetic solids and four-noded tetrahedron elements (SOLID96) for space. Six-noded trigonal prism elements (INFINI11) are used as infinite elements. SOURCE36 is used to model electric source. The geometrical information of the helical spring calculated by the superelastic deformation analysis program is transferred to the magnetic analysis program as solid modeling information (key-point and volume). The magnetic force increments are calculated at each node of the helical springs.

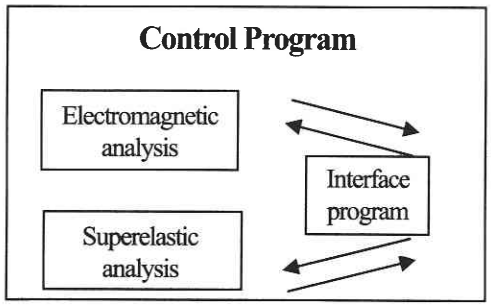

Fig. 1 Coupled magneto-superelastic analysis

2.2 Superelastic deformation analysis

The one-dimensional normal stress-normal strain relation is expressed by the following equation[3]:

$$\sigma - \sigma_0 = E(\varepsilon - \varepsilon_0) + \Omega(\xi_S - \xi_{S0}) + \theta(T - T_0) \quad \cdots\cdots (1)$$

where σ: stress, ε: strain, ξ_s: martensite volume fraction, T: temperature, E: Young's modulus, Ω: transformation tensor, ϑ: thermal elastic coefficient. The subscript '0' means the initial value.

The following equivalent stress of Drucker-Prager type[4] is used in the evolution equation for martensite volume fraction in order to consider the asymmetry of the tensile and compressive behavior:

$$\sigma_e = |\sigma| + 3\beta p \quad \cdots\cdots (2)$$

where β: material constant, p: pressure.

It is assumed that the shear stress-shear strain relation of SMA due to torsion is qualitatively similar to eq. (1), but they are independent with each other[5]. Then the shear stress-strain relation is expressed as

$$\tau - \tau_0 = G(\gamma - \gamma_0) + \Omega_\tau(\xi_{s\tau} - \xi_{s\tau 0}) \quad \cdots\cdots (3)$$

The evolution equation of the martensite volume fraction $\xi_{s\tau}$ due to torsion is assumed to be similar in form to that for the normal deformation. The equivalent stress is $\sqrt{3}|\tau_{\theta z}|$.

The followings are assumed in the finite element formulation using linear Timoshenko beam elements. The lateral deflections in two-directions, the rotation of the cross-section, the axial dis-

*Institute of Industrial Science, University of Tokyo
**University of Washington

placement and the torsional angle are all linearly interpolated in each element. The shear strain energy term due to bending is treated as a penalty term. The tangent modulus formulation by the total Lagrangian approach is conducted, considering superelasticity and large deformation. The nonlinear terms with respect to the axial displacement is neglected. Details of the formulation are given in Refs 1) and 2).

2.3 Interface program

As shown in Fig. 2, two-noded straight beam elements and eight-noded hexahedron solid elements are used in the superelastic deformation analysis and the magnetic analysis, respectively. Therefore, the data transformation for nodes and nodal forces is necessary in the coupled analysis.

The nodal coordinates on the N-th cross-section in Fig. 3 are given by the following equations:

$$\begin{aligned} x_N &= x_{N-1} + t a_{N-1} \\ y_N &= y_{N-1} + t b_{N-1} \\ z_N &= z_{N-1} + t c_{N-1} \end{aligned} \quad \cdots\cdots (4)$$

where

$$\begin{aligned} t = {} & a_{\frac{1}{2}}(X_N - x_{N-1}) / (a_{\frac{1}{2}} a_{N-1} + b_{\frac{1}{2}} b_{N-1} + c_{\frac{1}{2}} c_{N-1}) \\ & + b_{\frac{1}{2}}(Y_N - y_{N-1}) / (a_{\frac{1}{2}} a_{N-1} + b_{\frac{1}{2}} b_{N-1} + c_{\frac{1}{2}} c_{N-1}) \\ & + c_{\frac{1}{2}}(Z_N - z_{N-1}) / (a_{\frac{1}{2}} a_{N-1} + b_{\frac{1}{2}} b_{N-1} + c_{\frac{1}{2}} c_{N-1}) \end{aligned} \quad \cdots (5)$$

$$\begin{aligned} a_N &= (X_{N+1} - X_N) / T_N \\ b_N &= (Y_{N+1} - Y_N) / T_N \\ c_N &= (Z_{N+1} - Z_N) / T_N \\ T_N &= \sqrt{(X_{N+1} - X_N)^2 + (Y_{N+1} - Y_N)^2 + (Z_{N+1} - Z_N)^2} \end{aligned} \quad \cdot (6)$$

$$\begin{aligned} a_{\frac{1}{2}} &= (a_N + a_{N-1}) / T_{\frac{1}{2}} \\ b_{\frac{1}{2}} &= (b_N + b_{N-1}) / T_{\frac{1}{2}} \\ c_{\frac{1}{2}} &= (c_N + c_{N-1}) / T_{\frac{1}{2}} \\ T_{\frac{1}{2}} &= \sqrt{(a_N + a_{N-1})^2 + (b_N + b_{N-1})^2 + (c_N + c_{N-1})^2} \end{aligned} \quad \cdot (7)$$

In the equations, (X_N, Y_N, Z_N) is the global coordinates of the central node on the N -th cross-section. (x_N, y_N, z_N) is the global coordinates of the other nodes on the N -th cross-section.

The nodal forces F_{Nx}, F_{Ny}, F_{Nz} in the x, y, z -direction of the N -th node are calculated by the following equations:

$$F_{Nx} = \sum_{i=1}^{N_T} F_{ix}, \quad F_{Ny} = \sum_{i=1}^{N_T} F_{iy}, \quad F_{Nz} = \sum_{i=1}^{N_T} F_{iz} \quad \cdots\cdots (8)$$

where N_T is the total number of nodes on the N -th section. F_{ix}, F_{iy}, F_{iz} are the nodal forces at the i -th node in the x, y, z -direction. The nodal moments M_{Nx}, M_{Ny}, M_{Nz} in the x, y, z -direction of the N -th node are calculated by the following equations:

$$\begin{aligned} M_{Nx} &= \sum_{i=1}^{n} (l_{iy} F_{iz} - l_{iz} F_{iy}) \\ M_{Ny} &= \sum_{i=1}^{n} (l_{iz} F_{ix} - l_{ix} F_{iz}) \\ M_{Nz} &= \sum_{i=1}^{n} (l_{ix} F_{iy} - l_{iy} F_{ix}) \end{aligned} \quad \cdots\cdots (9)$$

where

$$l_{ix} = x_{Ni} - X_N, \quad l_{iy} = y_{Ni} - Y_N, \quad l_{iz} = z_{Ni} - Z_N \quad \cdots\cdots (10)$$

In eq. (10), (x_{Ni}, y_{Ni}, z_{Ni}) are the global coordinates of the i -th node on the N -th cross-section.

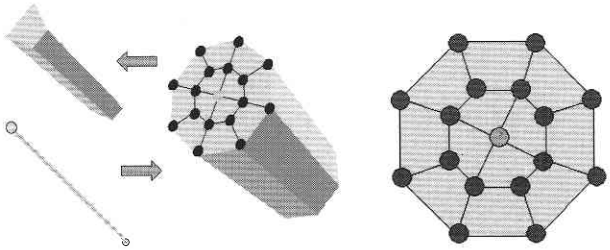

Fig. 2 Elements and cross-section

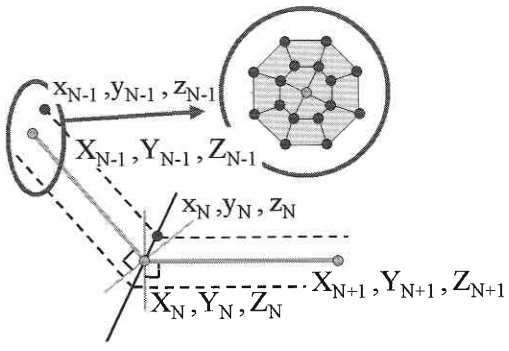

Fig. 3 Generation of nodes

4. Numerical Example

Fig. 4 shows a FePd helical spring with a weight subjected to magnetic force by the permanent magnet (Niodume35, 1.17, 835563A/m) and the electro-magnet (798 turns, 0~1.4A). Fig. 5 shows the dimensions of two-types of helical springs to be analyzed. Fig. 6 is B-H curves of FePd and york. The assumed stress-strain relation for FePd is shown in Fig. 7. The material constants are given in Table 1. The total number of elements for the magnetic analysis is 57067 (7 turns) and 89245 (10.5 turns). The total number of nodes (d. o. f.) is 10852 and 16599, respectively. The number of elements for the superelastic analysis is 88 (7 turns) and 130 (10.5 turns). The number of incremental steps is 8 for the magnetic analysis and 4500 for the superelastic analysis. Figs. 8 and 9 are the calculated results for current-displacement curves and deformations.

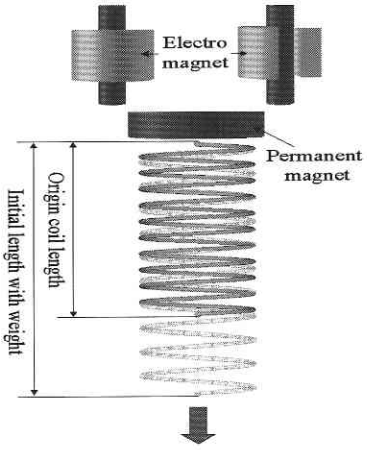

Fig. 4 FePd helical spring and magnets

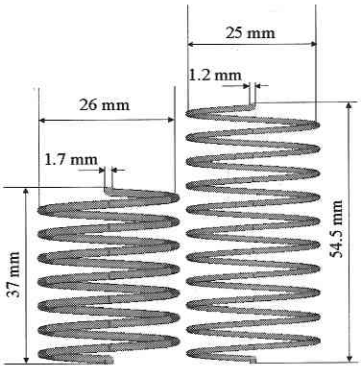

Fig. 5 FePd helical springs

Table 1 Dimensions and material constants

Dimensions (mm)	Material constants (MPa)
7 turns L =37 (Total length) d =1.7 (diameter) D =26 (Diameter)	$E_m = 49000,\ E_a = 53000$ $G_m = 16333,\ G_a = 17667$ $\sigma_{MS} = \sigma_s^{cr} + C_M(T - M_s) = 20$ $\sigma_{Mf} = \sigma_f^{cr} + C_M(T - M_s) = 560$ $\sigma_{AS} = C_A(T - A_s) = 18$ $\sigma_{Af} = C_A(T - A_f) = 2$
10.5 turns L =54.5 (Total length) d =1.2 (diameter) D =25 (Diameter)	$\varepsilon_L = \gamma_L = 0.001$ $\beta = 0.15$

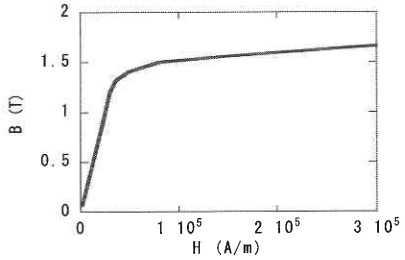

(a) FePd

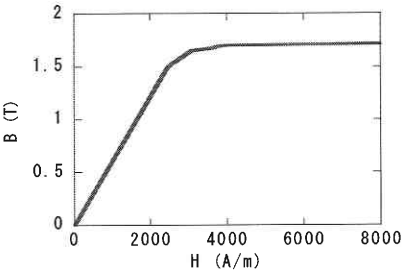

(b) yolk

Fig. 6 B-H curves

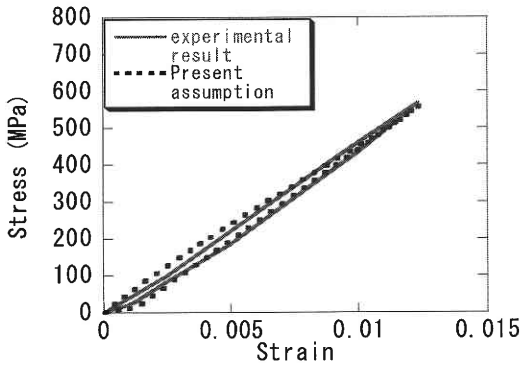

Fig. 7 Stress-strain curves for FePd

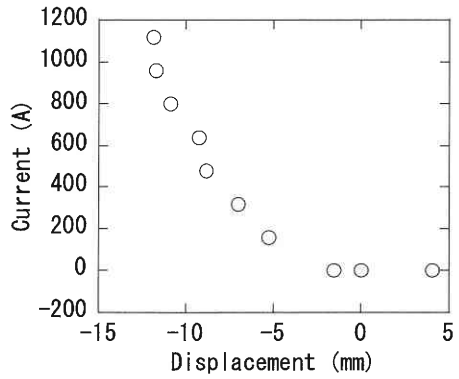

(a) helical spring with 7 turns

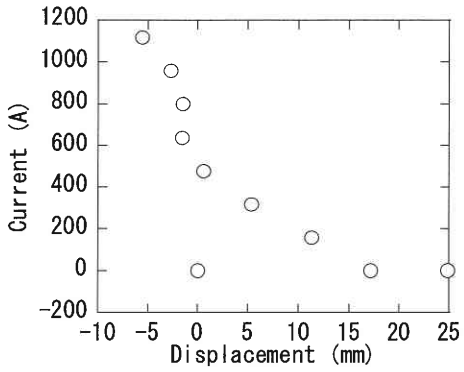

(b) helical spring with 10.5 turns

Fig. 8 Total current-displacement curves for FePd helical springs

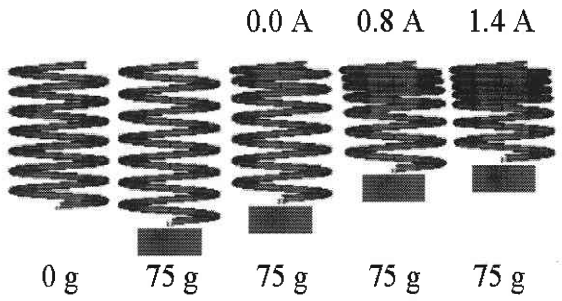

(a) helical spring with 7 turns

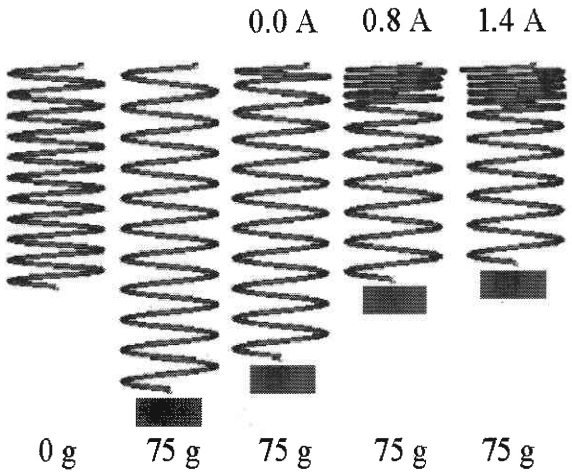

(b) helical spring with 10.5 turns

Fig. 9 Deformation of FePd helical springs

5. Concluding Remarks

The coupled finite element analysis is conducted for the magneto-superelastic behaviors of ferromagnetic shape memory alloy helical springs. Details of the constitutive equation and the finite element formulation are given in Ref. 1), 2) and 6). Quantitative discussion for the calculated results and experimental verification are future works.

(Manuscript received, August 5, 2003)

References

1) Toi, Y., Lee, J.-B. and Taya, M., Trans. Japan Soc. Mech. Engineers, 68–676, (2002), 1688–1694.
2) Toi, Y., Lee, J.-B. and Taya, M., *ibid.*, 68–676, (2002), 1695–1701.
3) Brinson, L. C., Journal of Intelligent Material Systems and Structures, (1993), 229–242.
4) Auricchio, F. and Taylor, R. L., Comput. Methods Appl. Mech. Engng, 143 (1997), 175–194.
5) Sun, Qing-Ping and Li, Zhi-Qi, Int. J. Solids Structures, 39 (2002), 3797–3809.
6) Toi, Y., Lee, J.-B. and Taya, M., Trans. Japan Soc. Mech. Engineers, (2003). submitted